Available online at www.sciencedirect.com
ScienceDirect
Journal of the European Ceramic Society 29 (2009) 629–635
www.elsevier.com/locate/jeurceramsoc

Titania ultrafiltration membrane: Preparation, characterization and photocatalytic activity

Ali Alem [a,*], Hossein Sarpoolaky [a], Mehrdad Keshmiri [b]

[a] *Department of Materials Science and Engineering, Iran University of Science and Technology, Tehran, Iran*
[b] *Department of Materials Engineering, University of British Columbia, Vancouver, Canada*

Received 14 March 2008; received in revised form 23 June 2008; accepted 9 July 2008
Available online 15 August 2008

Abstract

A mesoporous photocatalytic titania (TiO_2) membrane on alumina support is successfully fabricated via the sol–gel processing method. Several techniques such as dynamic light scattering, X-ray diffraction (XRD), TGA, N_2-sorption, and SEM are utilized to investigate the optimized processing parameters and their influence on the final properties of the developed membrane. The prepared titania sol containing organic additives (HPC and PVA) has an average particle size of 55.6 nm with a narrow distribution. The resulting TiO_2 membrane with thickness of 1 μm exhibits homogeneity with no cracks or pinholes. It also maintains small pore size (4.7 nm), large specific surface area (75 m^2/g), and small crystallite size (8.3 nm).

The permeability and photocatalytic properties of the titania membrane were measured. The permeability coefficient of the fabricated membrane is 30.09 $cm^3\ min^{-1}\ bar^{-1}\ cm^{-2}$. These measurements indicate an optimum processing condition for the preparation of the membrane. The prepared titania membrane has a great potential in developing high efficient water treatment and reuse systems because of its multifunctional capability such as decomposition of organic pollutants and physical separation of contaminants.

Keywords: Sol–gel processes; Electron microscopy; Porosity; Titania; Membranes; Photocatalytic activity

1. Introduction

Membranes play an important role in the separation technology, because membrane based separations are energy efficient and cost effective when optimized.[1] They represent promising alternatives to conventional water and waste water treatment processes. Among various types of membranes, ceramic membranes are widely used due to their numerous advantages, such as high temperature stability, high pressure resistance, good chemical stability, high mechanical resistance, long life and good anti-fouling properties.[2,3]

Researchers have explored various membrane preparation techniques such as state-particle-sintering,[4,5] sol–gel,[6,7] anodic oxidation,[8,9] chemical vapor deposition[10,11] and the reversed micelle method.[12,13] Among the various techniques, the sol–gel technique is considered to be one of the most practical methods for producing ceramic membranes, since it appears to be very precise, cost efficient and thus industrially a very effective technique.[14,15]

Alumina, titania and zirconia are considered as the most common porous ceramic membrane materials. Among ceramic membranes, TiO_2 photocatalysts have gained tremendous popularity, since a membrane skin layer composed of TiO_2 material has high water flux and chemical resistance, allows very small molecules and water to penetrate the membrane pores and its photocatalytic activity provides decomposition of toxic components in water.[16,17] The potential applications of titania membranes are numerous in the ultrafiltration process and in the catalytic/photocatalytic membrane reactor systems for liquid and gas separations.[18–20] During the photocatalytic process illuminated semiconductor absorbs light and generates active species, which leads to complete oxidation of organic components.[21]

The purpose of this investigation is to prepare a crack-free mesoporous titania membrane with desirable permeability and

* Corresponding author. Tel.: +98 21 88553581.
E-mail addresses: alialem59@gmail.com (A. Alem), hsarpoolaky@iust.ac.ir (H. Sarpoolaky), keshmiri@interchange.ubc.ca (M. Keshmiri).

0955-2219/$ – see front matter © 2008 Elsevier Ltd. All rights reserved.
doi:10.1016/j.jeurceramsoc.2008.07.003

photocatalytic properties using a sol–gel method. In this research several techniques are utilized to investigate the optimum processing conditions for the preparation of TiO_2 colloidal sol, layer deposition, and drying and calcination of the layer. Furthermore, this investigation examines the permeability and the photocatalytic properties of the prepared titania membrane. The precisely controlled fabrication procedure makes it possible to develop a nanostructured membrane with tailor-designed structure and multifunctional properties.

2. Experimental methods

2.1. Membrane preparation

In this section, the experimental procedures for the preparation of the alumina support and the titania layer are described thoroughly.

To prepare the support, Al_2O_3 granulate powder (KMS-92, Martinswerk) was shaped into a disk of 15 mm in diameter and 2 mm in thickness using a uniaxial press. The disks were pressed under the pressure of 31 Mpa. The sintering process was then performed at 1350 °C for 1 h.

The method used to prepare the titania colloidal sol and consequently to prepare the membrane layer, was the sol–gel technique. TiO_2 sol was obtained by hydrolysis of tetra isopropyl orthotitanate ($Ti(OC_3H_7)_4$) (Merck, 821895) via the addition of an excess H_2O ($[H_2O]/[Ti] > 4$). A solution of tetra isopropyl orthotitanate in isopropanol (Merck, 109634) was added dropwise to a solution of water in isopropanol while stirring at high speed. The hydrolysis product was filtered and then washed with water to remove the alcohol. The washed filtrate was redispersed in water to have Ti concentration of 5×10^{-4} mol/cm^3. The mixture was then electrostatically stabilized by HNO_3 and then was peptized at 50 °C for 1.5 h to create a stable titania sol. The sol was treated ultrasonically for 2 h to break the weakly agglomerated particles. Finally a stable semi-opaque titania sol was obtained through this processing method.

A solution of hydroxypropyl cellulose (HPC, Aldrich, 435007) with an average molecular weight of 80,000 (0.35 g/100 ml H_2O) and polyvinyl alcohol (PVA, Acros, 821038) with molecular weight of 88,000 (0.1 g/100 ml H_2O) were added to the sol as binders before coating the alumina support. The layer was formed by dip-coating the support in the prepared sol. The unsupported gel layer was also produced by pouring the prepared sol in a petri-dish.

The obtained gel layers were dried at room temperature for 24 h for both supported and unsupported layers. The drying process was continued in air for 1 h at 30 °C followed by 3 h at 40 °C. The membrane was subsequently calcined for 1 h at 450 °C by heating rate of 10 °C/h.

2.2. Characterization

The support porosity was measured by Archimedes method according to the ASTM 373-88 standard. The mechanical strength of the support was measured by SANTAM, STM-400 according to three-point bend test.

The particle size distribution of the sol was determined via the dynamic light scattering technique (Malvern, UK, 3000HSA). TGA technique was used in order to determine the burn out temperature of the organic additives and to examine the calcination conditions. The crystal structure and the phase transformation of the membrane layer during calcination process were identified using X-ray diffraction technique with Cu Kα wavelength (XRD, Jeol8000diffractometer). N_2-sorption measurement was performed (Micrometrics, Gemini 2375V4.02) to determine the BET surface area and the pore size of the unsupported titania layer. The membrane thickness, the surface quality of the layer, and the presence of any possible defect or crack on the layer were examined using the scanning electron microscope (PhillipsXL30).

2.3. Photocatalytic activity of the titania membrane

The photocatalytic activity of the prepared titania membrane was evaluated from the photocatalytic degradation of methyl orange in an aqueous solution. For this measurement, titania membrane was placed on a petri-box containing 30 ml of 5 mg l^{-1} aqueous solution of methyl orange. The membrane was then irradiated by a UV source (125 W, emission spectrum range of 360–415 nm) which has the maximum intensity of 370 nm (i.e. close to the anatase band gap). To measure the methyl orange concentration, the UV–visible spectrophotometer was used at the wavelength of 464 nm, which corresponds to the maximum adsorption of methyl orange. The change in the concentration of methyl orange was measured in presence of the titania membrane as a function of time.

2.4. Permeability of the membrane

The permeability of the prepared titania membrane was examined with a home-fabricated membrane chamber with a dead-end filtration type fitting the size and shape of the support.[22] This system has been established based on the ASTM S316 standard. The permeability of the membrane was determined by direct measurement of nitrogen permeate flow at 25 °C at trans-membrane pressure (TMP) from 0 to 3 bar.

3. Results and discussion

3.1. Support

Phase analysis of the alumina support after sintering shows that it only consists of α-Al_2O_3. We chose α-Al_2O_3 as a support material because it has a high chemical stability in strong acidic and basic environments.[23] In addition, since α-Al_2O_3 is prepared by sintering of Al_2O_3 powder, the support pore size would be large enough to build a pore size gradient from the support through the membrane layer. The gradient in the pore size effectively prevents early clogging of the membrane during its performance.

The mechanical strength of the support was measured to be 33 MPa according to the three-point bend test, which shows the

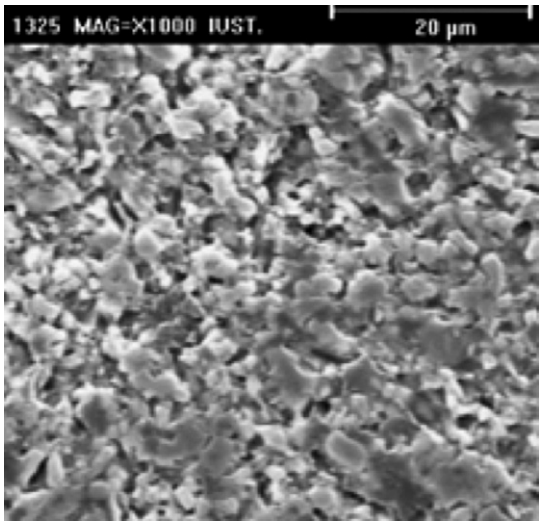

Fig. 1. SEM surface image of α-Al_2O_3 support, sintered at 1350 °C for 1 h, indicating a high porosity level in the support.

membrane to be highly reinforced by the alumina support. The measurements show the porosity of the support to be 38 per cent which is in agreement with its porous microstructure in Fig. 1.

3.2. Titania sol

The optimum experimental conditions for the sol synthesis are shown in Table 1. A suspension of nanometer-sized particles was obtained by reacting the precursor with a large excess of water. The concentration of water to Ti was kept at an optimum ratio (as shown in Table 1) to have a controlled hydrolysis reaction and to get smaller nanometer-sized particles.

Table 1
Optimum conditions for the preparation of stable titania colloidal sol

Type of the sol	Colloidal
$[H_2O]/[Ti]$	20
$[H^+]/[Ti]$	0.5
pH	1
Temperature (°C)	50

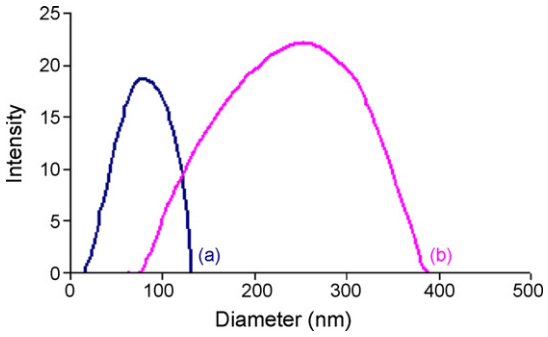

Fig. 2. The effect of pH on the sol particle size. (a) pH 1 and (b) pH < 1.

As Table 1 shows the sol optimum pH is equal to 1. Fig. 2 shows the effect of pH on the sol particle size. Graph (b) in this figure shows that at pH levels lower than 1, particle size distribution is too wide and the mean particle size is 245.4 nm. On the other hand, graph (a) in this figure shows that maintaining an optimum pH of 1 results in the formation of a stable and deflocculated sol with smaller nanometer-sized particles. At pH level of 1, sol consists of particles with a mean size of 55.6 nm and a minimum size of 19.7 nm. The figure also shows the sol particle size distribution to be narrow enough to result in a titania membrane with optimum properties. Although smaller particle size is more desirable to obtain enhanced membrane properties, it is not possible to stabilize particles for any small size required. As an example, in the case of TiO_2, the barrier for the particle size is approximately 10 nm.[24] In our experiment due to the presence of relatively large particles, the sol is semi-transparent. It should be noted that after the peptization process, the use of ultrasonic energy resulted in a narrow particle size distribution as well as a smaller particle size.

As discussed earlier in the experimental methods, hydroxypropyl cellulose (HPC) in combination with polyvinyl alcohol (PVA) was added to the sol before layer deposition. We observed that using PVA as a single additive causes flocculation of the titania sol, but in combination with HPC no flocculation occurs. HPC hinders the interaction between PVA and titania and therefore can prevent flocculation of the sol. Such additives have also been shown to adjust the viscosity of the sol, lower the sol surface tension and increase the strength of the unfired membrane layer.[25,26] Due to increased strength in the presence of HPC and PVA additives, the crack formation probability during the drying and calcination processes will be much lower.

Attempts to physically remove the titania layer from the alumina support suggest that the bond between the membrane and the support is adequate. This is because of the layer forming mechanism. In this research the layer forming mechanism is slip casting, because this mechanism exploits the capillary pressure exerted by the pores of the support which pulls the sol particles tightly onto the surface. One of the important advantages of the slip-casting process is that it leads to excellent adherence between the layer and the support. This unique property makes the membrane suitable for applications in which high back pressures are exerted on the layer. A homogenized structure can already be achieved during layer formation by slip-casting mechanism.[27]

It was observed that heating rate during the calcination step is also very important in producing a crack-free membrane. A controlled heating rate during the calcination step reduces the stresses originating from the burn out of the organic additives, the unequal thermal expansion coefficient of the support and the layer and also the layer shrinkage. In titania membranes, because of the spherically shaped titania particles, relaxation of the stresses that develop in the structure during drying and calcination steps, cannot easily take place. Therefore the heating rate should be slow enough to prevent cracking of the membrane.[27] As a result, one of the essential factors that prevents cracking of the membrane is to control the heating rate during the calcination process.

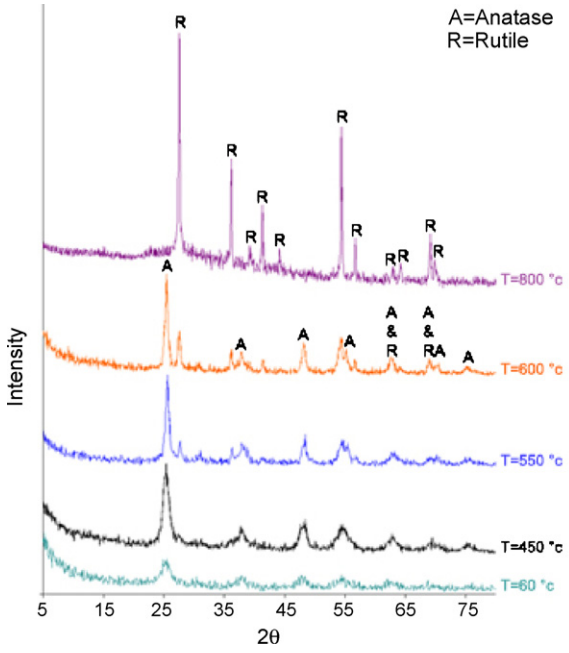

Fig. 3. XRD patterns of titania powder, calcined for 1 h at 60, 450, 550, 600, 800 °C. A: anatase peak and R: rutile peak.

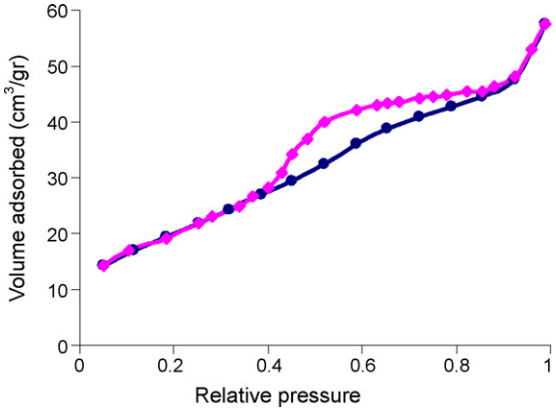

Fig. 4. N_2-sorption hysteresis for the mesoporous layer, calcined at 450 °C for 1 h.

Table 2
BET surface area and pore size of the titania unsupported membrane, calcined at 450 °C for 1 h

Type of material	Titania layer
Specific surface area (m^2/g)	75
Pore size (nm)	4.7

3.3. Titania membrane

3.3.1. Structural properties

According to the thermogravimetric results, the volatile materials in the layer such as nitric acid, the solvent and the organic additives are fully burned out below 400 °C.

Various values have been reported for the phase transformation temperature of titania in the literature.[28–30] The inconsistencies reported for the phase transformation temperature of titania clearly demand further investigations in order to achieve a better understanding of the effect of temperature along with other affecting parameters on the phase transformation of titania systems.

Fig. 3 shows the XRD patterns of the titania powder as a function of calcination temperature. According to this graph, at 450 °C titania is fully crystalline and is only in the anatase form. This figure also shows that the anatase to rutile phase transformation occurs at 550 °C. A few factors should be considered to select an optimum calcination temperature for the titania layer. First, the organic additives should be completely removed, and titania should remain crystalline with a minimal crystallite size. Moreover, titania should remain only in the anatase form after calcination. Considering the above factors, XRD in combination with TGA results show the optimum calcination time and temperature for the titania membrane to be 1 h and 450 °C, respectively. The low calcination temperature of titania makes it possible to prepare membranes with reduced pore and crystallite sizes.

According to the Scherer's equation[31] at peak (1 0 1), the crystallite size of titania, calcined for 1 h at 450 °C was determined to be 8.3 nm. The optimum crystallite size for anatase in order to get the highest possible photoactivity is in the range 8–10 nm.[32] This range provides the best photoactivity for the membrane which will be discussed later in Section 3.3.3 of this paper (the photocatalytic properties of the membrane).

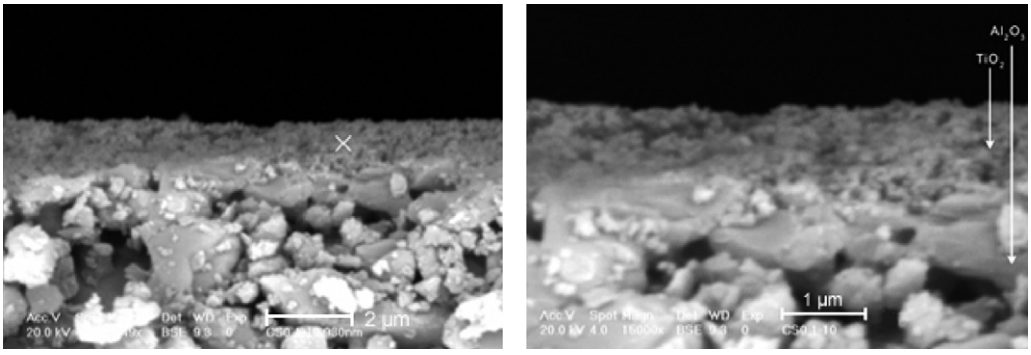

Fig. 5. SEM cross-section image of the titania membrane, calcined at 450 °C for 1 h.

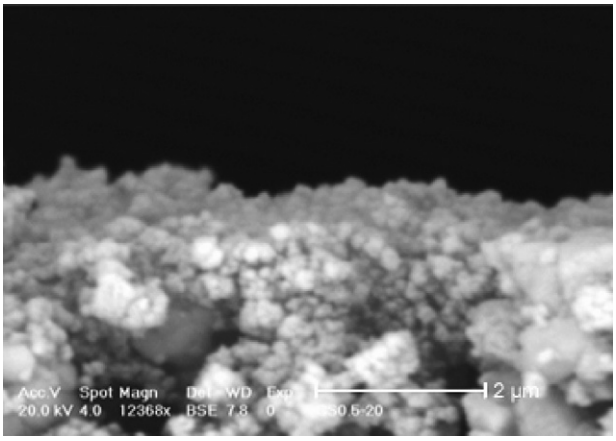

Fig. 6. SEM cross-section image of the rough titania layer, calcined at 450 °C for 1 h.

Table 2 shows the results of N_2-sorption measurements. This technique was performed to determine specific surface area and pore size of the unsupported membrane. The specific surface area and the pore size were measured 75 m^2/g and 4.7 nm, respectively. Fig. 4 shows the N_2-sorption hysteresis of the membrane which is in agreement with the measured pore size. It shows that the prepared membrane is mesoporous.[33] The specific surface area measurement was based on the BET model and the pore size was characterized based on the assumption of cylindrical pores.[34–36]

3.3.2. Microstructure

Fig. 5 shows the SEM cross-section images of the prepared titania membrane. As the figure shows the thickness of the titania layer is about 1 μm. This figure also shows formation of a smooth and crack-free titania layer on top of the alumina support.

Figs. 6 and 7 show the effect of thickness on the surface quality and roughness of the layer. The layer tends to become rough and defective, when the layer thickness is smaller than the optimum thickness (Fig. 6). In contrast, when the layer thickness is larger than its optimum size, the layer is more likely to crack during the drying and calcination processes (Fig. 7). Our studies show that the optimum thickness is 1 μm that provides a uniform and crack-free layer (Fig. 5). Furthermore, an optimum layer thickness can increase the photocatalytic properties of the membrane, which will be discussed later in the photocatalytic properties of the membrane (Section 3.3.3).

Table 3
Photocatalytic properties of the prepared titania membrane, calcined at 450 °C for 1 h

Type of the titania membrane	Membrane with one colloidal layer
Decomposition after 3 h UV radiation (per cent)	15.8
Decomposition after 6 h UV radiation (per cent)	20
Decomposition after 9 h UV radiation (per cent)	27.1

Our observations show that the layer thickness increases with increasing the sol concentration and the dipping time. It was also observed that the dipping time of 30 s is necessary to form a defect-free titania layer.

The stresses generated during the anatase to rutile phase transformation can cause severe cracking of the membrane. According to Fig. 3, in this study the anatase to rutile phase transformation was inhibited by selecting an optimum calcination temperature of 450 °C. Therefore, the cracks in Fig. 7 are caused due to the high levels of stress generated only by the large layer thickness (2 μm).

3.3.3. Photocatalytic properties

Table 3 shows the photocatalytic properties of the prepared titania membrane. This table shows that the degradation of methyl orange is highly affected by UV radiation time. As discussed earlier in the experimental chapter, a small-sized membrane with a diameter of 15 mm has been chosen for this investigation. As a result the contact surface between the membrane and the solution is small. In spite of the fact that the membrane maintains a relatively small surface contact with the solution, the photocatalytic test indicates that the degradation of methyl orange is desirable. Therefore the TiO_2 photocatalyst immobilized onto a thin membrane has a high photocatalytic activity per unit mass of the catalyst. This high photocatalytic activity also points to the precise processing conditions in this investigation.

For comparison, the methyl orange solution was also irradiated in the absence of photocatalyst to examine its stability.

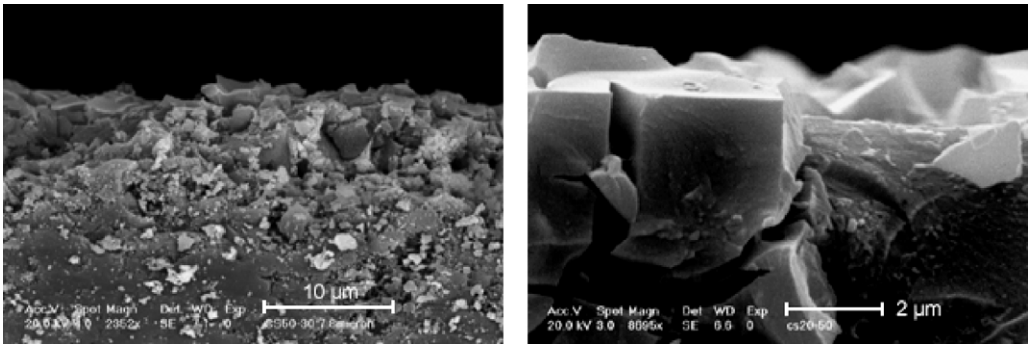

Fig. 7. SEM cross-section image of the cracked titania layer, calcined at 450 °C for 1 h.

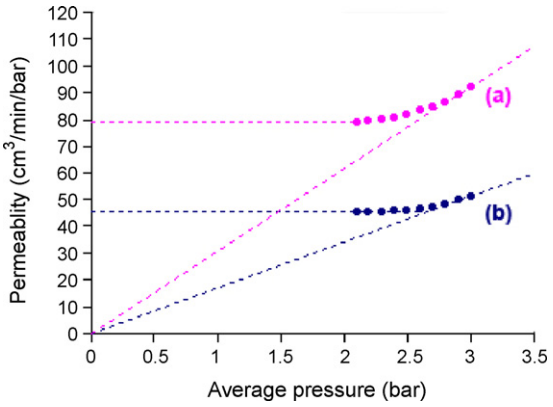

Fig. 8. Permeability of the membrane, (a) support (b) support and layer.

In this case, the results verify that the organic compound is not decomposed even after long UV irradiation time.

In our study, we observed that the calcination time and temperature strongly affect the photocatalytic properties of the membrane. Increasing the calcination time and temperature causes an increase in the particle size and a decrease in the specific surface area and the crystallite size. They can also increase the amount of rutile phase present in the titania layer which lowers the photocatalytic activity.[37,38]

A high specific surface area can reduce volume electron–hole recombinations and can increase the number of active sites on the surface of the photocatalyst. An increase in the number of active sites on the surface of the photocatalyst clearly leads to a faster rate for electron–hole reactions with the surrounding substrate. As a result, the photoactivity of the photocatalyst is enhanced by increasing the specific surface area of the photocatalyst. It should be noted that the photocatalytic efficiency of the membrane does not increase monotonically with increasing the surface area. This is due to the fact that the surface recombination of charge carriers becomes an important process in the photocatalytic reactions in the ultrafine particles.[39,40] Therefore, the results of this investigation show that the photocatalytic activity of titania is strongly dependent on its phase structure, crystallite size, and specific surface area.

We also observed that the membrane thickness affects its photocatalytic properties. Increasing the film thickness can bring better results with respect to the adsorption capacity and the photocatalytic activity of the film. However, it also increases the preparation time and the fabrication cost. Increasing the layer thickness correlates with the amount of photocatalyst immobilized on the support and thus the amount of methyl orange absorbed onto the photocatalyst.[1] But considering Fig. 7 which shows cracks because of the high layer thickness, it is obvious that the membrane must have its optimum thickness.

3.3.4. Permeability

Permeability of the membrane was measured to evaluate the integrity and the properties of the membrane, as shown in Fig. 8. Graph (a) of this figure clearly shows that the support has a high permeability. On the other hand, the permeability of the membrane with a thickness of 1 μm exhibited a considerable decrease, compared to the alumina support. This experiment shows a decrease in the permeability coefficient from 52.61 ($cm^3\ min^{-1}\ bar^{-1}\ cm^{-2}$) for the alumina support to 30.09 ($cm^3\ min^{-1}\ bar^{-1}\ cm^{-2}$) for the titania membrane. The lower permeability of the membrane is explained by its small pore size. The horizontal part in graph b of Fig. 8 reveals the significant contribution of the Knudsen diffusion. Knudsen diffusion plays an important role in a mesoporous membrane with a small pore size. In this region the membrane permeability is independent of the applied pressure.[41] Therefore, this Knudsen diffusion clearly confirms the hysteresis in Fig. 4. These measurements exhibited that increasing the layer thickness via multi-coating procedure can decrease the permeability and increase the possibility for crack formation.[1]

4. Conclusion

A crack-free nanostructured titania membrane was successfully fabricated via the sol–gel process. The controlled synthesis route resulted in a membrane with promising structural properties such as homogeneity, large surface area (75 m^2/g), and small pore size (4.7 nm). This synthesis process also led to desirable photocatalytic properties such as active anatase phase, small crystallite size (8.3 nm), and high material crystallinity. This study also indicated that the membrane thickness, and its calcination time and temperature strongly affect the photocatalytic activity of the membrane.

In the single-coating procedure via a sol with optimum concentration and properties, the preparation time and cost were reduced without sacrificing the membrane permeability and photocatalytic activity. The prepared photocatalytic membrane with optimum thickness of 1 μm has great implication for environmental applications due to its simultaneous photocatalytic, disinfection, and separation functions.

We are currently investigating the methods to improve the separation function and photocatalytic activity of the titania membrane without decreasing its permeability. This sol–gel method is useful for the preparation of nanostructured titania membranes with high photocatalytic activity and desirable permeability.

References

1. Choi, H., Stathatos, E. and Dionysiou, D. D., Sol–gel preparation of mesoporous photocatalytic TiO_2 films and TiO_2/Al_2O_3 composite membranes for environmental applications. *J. Appl. Catal. B: Environ.*, 2006, **63**, 60.
2. Bhave, P. R., *Inorganic Membrane Synthesis, Characteristics and Applications*. Van Nostrand Reinhoild, New York, 1991.
3. Burggraaf, A. J. and Cot, L., *Fundamentals of inorganic membrane science and technology*. Elsevier, 1966.
4. Auriol, A. and Tritten, D., A process for the manufacture of porous supports. French Patent 2,463,636 (1973).
5. Terpstra, R. A., Bonekamp, B. C. and Veringa, H. G., Preparation, characterization and some properties of tubular alpha alumina ceramic membranes for microfiltration and as a support for ultrafiltration and gas separation membranes. *J. Desalinat.*, 1988, **70**, 395.
6. Leenaars, A. F. M. and burggraaf, A. J., the preparation and characterization of alumina membranes with ultra fine pores. Part 2. The formation of supported membranes. *J. Colloid Interface Sci.*, 1985, **105**, 27.

7. Klein, L. C. and Gallagher, D., Pore structures of sol–gel silica membranes. *J. Membr. Sci.*, 1988, **39**, 213.
8. Hoar, T. P. and Mott, N. M., Mechanism for the formation of porous anodic oxide films on aluminum. *J. Phys. Chem. Solids*, 1959, **9**, 97.
9. Smith, A. W., Porous anodic alumina oxide membrane. *J. Electochem. Soc.*, 1973, **120**, 1068.
10. Lin, Y. S. and Burggraaf, A. J., Modeling and analysis of CVD processes in porous media for ceramic composite preparation. *J. Chem. Eng. Sci.*, 1991, **46**, 3067.
11. Lin, Y. S. and Burggraaf, A. J., CVD of solid oxides in porous substrates for ceramic membrane modification. *AIChE J.*, 1992, **38**, 445.
12. Yamaki, T., Maeda, H., Kusakabe, K. and Morooka, S., Control of the pore characteristics of thin alumina membranes with ultrafine zirconia particles prepared by the reversed micelle method. *J. Membr. Sci.*, 1993, **85**, 167.
13. Ju, X. S., Huang, P., Xu, N. P. and Shi, J., Studies on the preparation of mesoporous titania membrane by the reversed micelle method. *J. Membr. Sci.*, 2002, **202**, 67.
14. Yordanova, V., Stabova, K., Hintz, W., Tomas, J. and Wendt, U., Excimer laser induced photo-thermal changes of sol–gel TiO_2 thin films. *J. Optoelectron. Adv. Mater.*, 2005, **7**, 2601.
15. Brinker, C. J., *Sol–gel Science: The Physics and Chemistry of Sol–Gel Processing*. Harcourt Brace Jovanovich, Boston, 1990.
16. Zaspalis, V. T., Praaq, W. V., Keizer, K., Ommen, J. G. V., Ross, J. R. H. and Burggraaf, A. J., Reactor studies using vanadia modified titania and alumina catalytically active membranes for the reduction of nitrogen oxide with ammonia. *J. Appl. Catal.*, 1991, **74**, 249.
17. Hyun, S. J. and Kang, B. S., Synthesis of titania composite membranes by the pressurized sol–gel technique. *J. Am. Ceram. Soc.*, 1997, **79**, 279.
18. Larbot, A., Fabre, J.-P., Guizard, C., Cot, L. and Gillot, J., New inorganic ultrafiltration membranes: titania and zirconia membranes. *J. Am. Ceram. Soc.*, 1989, **72**, 257.
19. Xu, Q. and Anderson, M. A., Sol–gel route to synthesis of microporous ceramic membranes: thermal stability of TiO_2-ZrO_2 mixed oxides. *J. Am. Ceram. Soc.*, 1993, **76**, 2093.
20. Chang, C. H., Gopalan, R. and Lin, Y. S., A comparative study on thermal and hydrothermal stability of alumina, titania and zirconia membranes. *J. Membr. Sci.*, 1994, **91**, 27.
21. Dobosz, A. and Sobczynski, A., The influence of silver additives on titania photoactivity in the photooxidation of phenol. *J. Water Res.*, 2003, **37**, 1489.
22. Falamaki, C., Aghaei, A. and Ardestani, N. R., Iranian Patent 26,446 (2000).
23. Tsuru, T., Hironaka, D., Toshioka, T. and Asaeda, M., Titania membranes for liquid phase separation: effect of surface charge on flux. *J. Sep. Purif. Technol.*, 2001, **25**, 307.
24. Puhlfurß, P., Voigt, A., Weber, R. and Morbe, M., Microporous TiO_2 membrane with a cut off <500 Da. *J. Membr. Sci.*, 2000, **174**, 123.
25. Sekulić-Kuzmanović, J., Mesoporous and Microporous Titania Membranes, Thesis, 2004.
26. Larbot, A., Fabre, J. P., Guizard, C. and Cot, L., Inorganic membrane obtained by sol–gel techniques. *J. Membr. Sci.*, 1988, **39**, 203.
27. Zaspalis, V. T., Praag, W. V., Keizer, K., Ross, J. R. H. and Burggraaf, A. J., Synthesis and characterization of primary alumina, titania and binary membranes. *J. Mater. Sci. Catal.*, 1992, **27**, 1023.
28. Kumar, K. P., Zaspalis, V. T., Keizer, K. and Burggraaf, A. J., Drying process in the formation of sol–gel-derived TiO_2 ceramic membrane. *J. Non-crystalline Solids*, 1992, **147&148**, 375.
29. Ding, X., Fan, Y. and Xu, N., A new route for the fabrication of TiO_2 ultrafiltration membranes with suspension derived from a wet chemical synthesis. *J. Membr. Sci.*, 2006, **270**, 179.
30. Peterson, R. A., Webster, F. T., Niezyniecki, G. M., Anderson, M. A. and Hill, C. G., Ceramic membranes for navel separations. *J. Sep. Sci. Technol.*, 1995, **30**, 1689.
31. Cullity, B. D., *Elements of X-ray Diffraction* (*2nd ed.*). Addison-Wesley, 1978.
32. Bosc, F., Ayral, A., Albouy, P. and Guizard, C., A simple route for low-temperature synthesis of mesoporous and nanocrystalline anatase thin films. *J. Chem. Mater.*, 2003, **15**, 2463.
33. Koros, W. J., Ma, Y. H. and Shimidzu, T., Terminology for membranes and membrane process, IUPAC; Commission on membrane nomenclature, 1995.
34. Saito, A. and Foley, H. C., Curvature and parametric sensitivity in models for adsorption in micropores. *AICHE J.*, 1991, **37**, 429.
35. Gregg, S. J. and Sing, K. S. W., *Adsorption, surface area and porosity* (*2nd ed.*). Academic Press, 1982.
36. Sing, K. S. W., Everett, D. H., Haul, R. A. W., Moscou, L., Pierotti, R. A., Rouquerol, J. and Siemieniewska, T., Reporting physisorption data for gas/solid systems with special reference to the determination of surface area and porosity. *J. Pure Appl. Chem.*, 1985, **57**, 603.
37. Rajeshwar, K., Photoelectrochemistry and the environment. *J. Appl. Electrochem.*, 1995, **25**, 1067.
38. Schindler, K. M. and Kunst, M., Charge carrier dynamics in TiO_2 powders. *J. Phys. Chem.*, 1990, **94**, 8222.
39. Wade, J., *An Investigation of TiO_2–$ZnFe_2O_4$ nanocomposites for Visible Light Photocatalysis*. University of South Florida, 2005.
40. He, C., Yu, Y., Hu, X. and Larbot, A., Influence of silver doping on the photocatalytic activity of titania films. *J. Appl. Surf. Sci.*, 2002, **200**, 239.
41. Baker, R. W., *Membrane Technology and Applications* (*2nd ed.*). John Wiley and Sons, 2004.